Enhancing Light Efficiency and Moisture Stability of the Quantum Dots-Light-Emitting Diodes by Coating Superhydrophobic Nanosilica Particles

Xingjian Yu, Naiqi Pei, Shuling Zhou, Xiaoyu Zhang, and Xiaobing Luo, *Fellow, IEEE*

***Abstract*— Quantum dots-light-emitting diodes (QDs-LEDs) have attracted extensive attention in recent years due to their outstanding performance of color-rendering index (CRI). QDs were found to undergo severe fluorescence quenching in moisture environments, while rare solutions were proposed to solve this issue. In this article, 1H,1H,2H,2H-perfluorooctyltrichlorosilane (FOTS)-modified superhydrophobic nanosilica (FOTS-NS) particles were synthesized and coated on the QDs/polymer films to prevent the moisture from penetrating the films. The light efficiency of the FOTS-NS-coated LEDs was investigated, and the moisture stability of the FOTS-NS-coated QDs/polymer films was tested in an extreme moisture environment (50 °C, 99.6% relative humidity) for 270 h. The results show that compared with the uncoated LEDs, the FOTS-NS layer increases the light efficiency by ∼10% for the blue LEDs and ∼3.8% for the white LEDs (correlated color temperature of ∼5000 K and Ra of ∼91) by optimizing the particle deposition density of the FOTS-NS. Besides, the normalized peak intensity degradation of QDs embedded in the coated and uncoated films after aging for 270 h is ∼35.68% and ∼77.66%, showing the capacity of FOTS-NS layer on enhancing the moisture stability of the QDs-LEDs.**

***Index Terms*— Light efficiency, moisture stability, quantum dots-light-emitting diodes (QDs-LEDs), superhydrophobic nanosilica (NS).**

I. Introduction

WHITE light-emitting diodes (LEDs) are the most popular lighting source in the 21st century and have gradually replaced the traditional incandescent and fluorescent lamps in many lighting fields [1]. Nowadays, the most common commercial white LEDs are realized by coating phosphors [2]–[4] on the LED chip, which is well-known as phosphor-converted LEDs (pc-LEDs) [5]–[7]. The pc-LEDs present extremely high light efficiency and reliability over high temperature and moisture environment. However, they suffer low color-rendering index (CRI) (typically Ra $<$ 80) due to the wide full-width at half-maximum (FWHM) of the phosphor and the lack of red and green spectral components [8], [9], which hinders their further application in many lighting fields such as backlight display and mobile phones.

Quantum dots (QDs) have attracted extensive attention in solid-state lighting (SSL) in recent years due to its narrow emission spectra and high quantum yields. Numerous studies show that the white LEDs with Ra $>$ 90 can be easily realized by adding green or red QDs into the conventional pc-LEDs [10]–[13]. Although the QDs-LEDs have higher CRI, they suffer more serious thermal and moisture stability problems than the conventional pc-LEDs [14]–[17]. The presence of oxygen and/or moisture leads to the aggregation, surface destruction, and active layer degradation of the QDs, which induces severe fluorescence quenching, spectra change, and even device failure [18], [19]. Therefore, it is of great importance to isolate oxygen and moisture from the QDs. Few methods were proposed to achieve this goal including mesoporous silica embedding [20]–[24], polymer coating [polyvinyl alcohol (PVA) and polymethylmethacrylate (PMMA), etc.] [25]–[27], and siloxane encapsulating [28], [29]. However, these methods involve complex material synthesis processes and may induce quantum yield drop of QDs, depending on the optical properties of the materials used.

In current QDs-LEDs packaging, the pristine QDs are mixed with curable polymer materials (silicone, PMMA, etc.) to form the QDs/polymer film to keep the QDs away from oxygen and moisture [30], [31]. Indeed, this can retard the fluorescence quenching of QDs under low moisture environment. However, a previous study showed that the moisture can penetrate into the polymer film when the film was exposed to extreme moisture environment for a long time [32]. Therefore, it is predictable that the QDs/polymer film will also undergo severe fluorescence quenching in extreme moisture environment. However, researches on the moisture stability

Manuscript received September 11, 2019; revised October 4, 2019; accepted October 11, 2019. Date of publication November 5, 2019; date of current version November 27, 2019. This work was supported in part by the National Natural Science Foundation of China under Grant 51625601, Grant 51576078, and Grant 51606074, in part by the Ministry of Science and Technology of the People's Republic of China under Project 2017YFE0100600, and in part by the Creative Research Groups Funding of Hubei Province under Grant 2018CFA001. The review of this article was arranged by Editor C. Bayram. *(Corresponding author: Xiaobing Luo.)*

The authors are with the School of Energy and Power Engineering, Huazhong University of Science and Technology, Wuhan 430074, China (e-mail: luoxb@hust.edu.cn).

Color versions of one or more of the figures in this article are available online at http://ieeexplore.ieee.org.

Digital Object Identifier 10.1109/TED.2019.2947335

of the QDs/polymer film are almost blank. Hence, it is of great importance to investigate the moisture stability of the QDs/polymer film and find solutions to enhance it.

In recent years, surperhydrophobic surfaces with hierarchical structure have been extensively studied and applied to numerous applications, such as self-cleaning, corrosion prevention, and chemical shielding [33]. The low surface functionalized hierarchical structures have been proven to effectively prevent moisture from penetrating the interior of the surfaces [33]. Thereby, we assumed that this method can be applied to isolate the moisture from the QDs/polymer film. The main challenge is how to realize the transparent superhydrophobic surfaces to ensure the light extraction efficiency of the QDs/polymer film. Fortunately, the random aggregation of the transparent nanosilica (NS) particles can be an alternative method to realize such surfaces [34], [35].

The aim of this article is to investigate the moisture stability of the QDs/polymer films and find solution to enhance it. To achieve this goal, we built a moisture reliability test experimental setup. The red-emissive CdSe/ZnS core/shell QDs were synthesized [36] and mixed with silicone to form the QDs/polymer films. To enhance the moisture stability of the QDs/polymer films, the superhydrophobic NS particles were prepared and coated on the QDs/polymer films to prevent the moisture from penetrating the films. The morphology, wettability, and stability of the coated surfaces were characterized. The light efficiency and the moisture stability of the QDs-LEDs with coated and uncoated films were investigated.

II. Methodology

A. Fabrication of the Transparent Superhydrophobic Surfaces

The transparent NS particles were chosen to realize hierarchical structure. However, the high surface energy of pristine NS and the presence of the hydroxyl (−OH) in pristine NS make the NS particles present superhydrophilic wettability. Therefore, the pristine NS should be low surface-energy-modified. The superhydrophobic NS particles were prepared by our previous proposed method as shown in Fig. 1 [37]. First, the pristine NS particles were synthesized by hydrolyzing the tetraethoxysilane (TEOS), then the pristine NS particles were modified with 1H,1H,2H,2H-perfluorooctyltrichlorosilane (FOTS), and the FOTS-modified NS particles were called as FOTS-NS in subsequent description. The morphology of the nanoparticles was characterized by transmission electron microscope (TEM, Tecnai-G20, FEI). The prepared NS and FOTS-NS particles were dispersed in ethanol and deposited on the glass substrate to characterize the wettability of the nanoparticles and the transparency of the FOTS-NS-coated layer.

B. Light Efficiency Characterization of the FOTS-NS-Coated LEDs

As shown in Fig. 2(a), the chip-on-board LED module with 2 × 2 chip array was used in the experiments. First, the phosphor–QDs/polymer mixture was coated on the LED module by the direct dispensing method to form a thin flat film above the LED chip as shown in Fig. 2(b). After the film was cured, the FOTS-NS particles were deposited on the top surface of the film by the spray coating method as shown in Fig. 3(c). The morphology of the coated surfaces was characterized by scanning electron microscope (SEM, JSM-7600F, JEOL).

In the experiments, the blue LED modules and the white LED modules with correlated color temperature (CCT) of ∼5000 K were fabricated. For the blue LED modules, only silicone was coated on the LED modules. For the white LED modules, the phosphor–QDs/polymer mixture was used and the concentration of the phosphor–QDs was adjusted to generate the desired CCT, and the mass ratio of each component was set as 0.075 g phosphor:0.25 mg QDs:1 g silicone. The red-emissive CdSe/ZnS core/shell QDs were synthesized and used. Yellow phosphor (YAG-O4, Intematix)

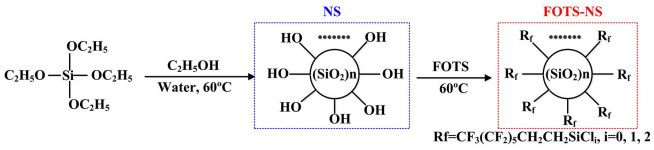

Fig. 1. Synthesize process of the surperhydrophobic NS particles.

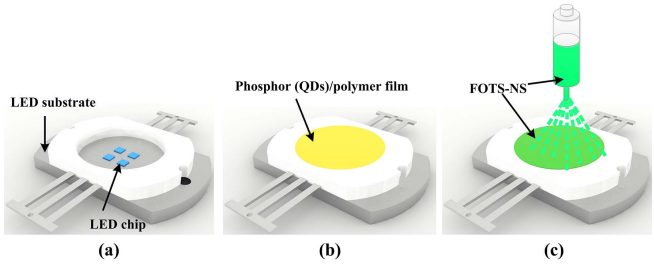

Fig. 2. Fabrication process of the FOTS-NS-coated LEDs. (a) Structure of the LED modules used in the experiments. (b) Coating phosphor (QDs)/polymer film. (c) Coating FOTS-NS particles.

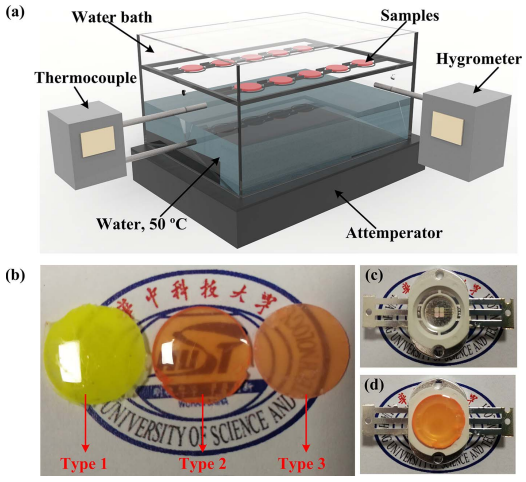

Fig. 3. Moisture characterization. (a) Experimental setup. (b) Image of the three types of samples. (c) LED module used in the experiments. (d) LED module with remote QDs.

was used because white light cannot be generated with red QDs solely. Silicone (OE6550A/B, Dow corning) was used as the polymer to disperse the phosphor and QDs.

To characterize the effect of the FOTS-NS particle coating on the light efficiency of the LEDs, the particle deposition density (PDD) was adjusted from 0 to 9 g/m^2. To enhance the adhesion of the nanoparticle to the film, silicone was used as the binder during the spraying coating process. The light efficiency of the LED modules was measured with an integrating sphere (ATA-1000, Everfine).

C. Moisture Stability Characterization of the Coated and Uncoated Films

An experimental setup as shown in Fig. 3(a) was established to explore the moisture stability of the coated and uncoated films. All the samples were placed in a water bath with size of 150 mm × 120 mm × 65 mm. The depth of the water was 25 mm and the samples were placed at 50 mm from the bottom. Two thermocouples were used to monitor the temperature of the water and the temperature around the samples. A hydrometer was applied to monitor the relative humidity around the samples. Two small holes were opened at the side surfaces of the water bath to keep the pressure inside the water bath consistent with the atmospheric pressure. An attemperator was applied to heat the water to 55 °C ± 1 °C by adjusting the input power. The water evaporates after being heated to form a high moisture environment in the upper space of the water bath. The temperature and relative humidity around the sample were measured as 50 °C and 99.6%, respectively.

Three types of samples as shown in Fig. 3(b) were prepared: 1) type 1: phosphor/polymer film with the mass ratio of 0.075 g phosphor:1 g silicone; 2) type 2: QDs/polymer film with the mass ratio of 0.25 mg QDs:1 g silicone; and 3) type 3: FOTS-NS-coated QDs/polymer film with the mass ratio of QDs consistent with type 2 and the FOTS-NS particles cover the entire surface of the film. The diameter and the thickness of the films were set as 12.7 mm ± 0.2 mm and 1 mm ± 0.05 mm, respectively, and five samples were prepared for each type. The wettability and stability of the FOTS-NS-coated films over temperature and time were characterized. To eliminate the impact of moisture on the stability of other components of the LED module, only the films were placed inside the water bath. For the light efficiency test, the films were taken out of the bath and put on the LED module as shown in Fig. 3(c) with a remote structure as shown in Fig. 3(d). The spectra and peak intensity of the phosphor and QDs over aging time of 270 h were measured and analyzed.

III. Results and Discussion

Fig. 4(a) shows the TEM image of the FOTS-NS particles. It shows that the FOTS-NS particles present spherical morphology with a diameter of ∼70 nm. The NS and FOTS-NS particles were deposited onto a 1-mm glass substrate with the PDD of 0.5 g/m^2 to characterize their wettability difference and the result is shown in Fig. 4(b) and (c). The NS-coated surface presents superhydrophilic property due to the presence of hydroxyl (−OH), while the FOTS-NS-coated surface presents superhydrophobic property because the low surface energy functional group ($-CH_2CH_2(CF_2)_5CF_3$) replaces the hydroxyl (−OH). More detailed characterization of the nanoparticles can be obtained from our previous studies [37], [38].

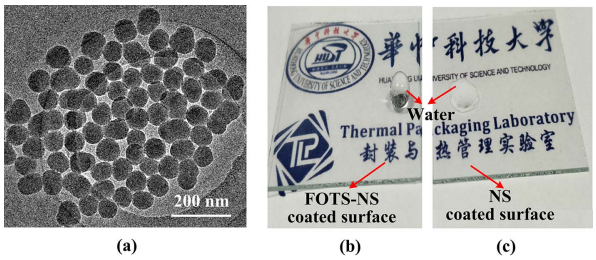

Fig. 4. Morphology and wettability of the particles. (a) TEM image of the FOTS-NS particles. (b) Wettability of the FOTS-NS- and (c) NS-coated surfaces.

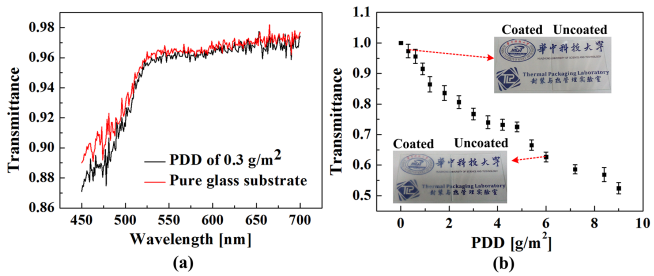

Fig. 5. Transparency characterization results of the FOTS-NS layer. (a) Transmittance of pure glass substrate and FOTS-NS-coated substrate with the PDD of 0.3 g/m^2 at wavelength from 450 to 700 nm. (b) Transmittance of the FOTS-NS layer with the PDD from 0 to 9 g/m^2.

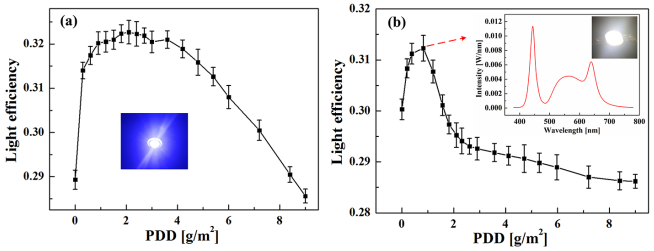

Fig. 6. Light efficiency of the FOTS-NS-coated LEDs with PDD from 0 to 9 g/m^2. (a) Blue LEDs. (b) White LEDs with CCT of ∼5000 K and Ra of ∼91.

Fig. 4(b) also shows that the FOTS-NS-coated surfaces present high transparency, which indicates the application feasibility of the FOTS-NS particles in LED packaging. Fig. 5(a) shows the transmittance of the pure glass substrate and the FOTS-NS-coated substrate with the PDD of 0.3 g/m^2 at a wavelength from 450 to 700 nm. The transmittance of the two substrates is approximated at all wavelengths. Fig. 5(b) shows the transmittance of the FOTS-NS layer with the PDD from 0 to 9 g/m^2, and the transmittance of the FOTS-NS layer is defined as the transmittance ratio of the coated substrate to the uncoated substrate. The results indicate that the transmittance of the FOTS-NS layer decreases with the PDD monotonically.

Fig. 6 shows the light efficiency of the FOTS-NS-coated blue and white LEDs with the PDD of 0–9 g/m^2; all the

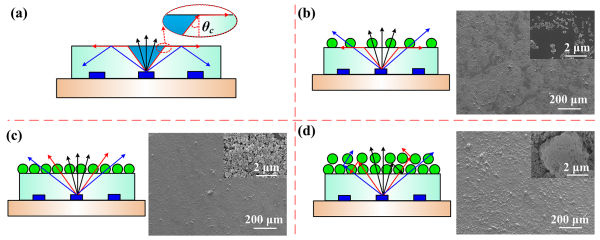

Fig. 7. Schematic light propagation at the silicone–air interface and the morphology of nanoparticles under different PDDs. (a) 0 g/m^2. (b) 0.3 g/m^2. (c) 0.9 g/m^2. (d) 3 g/m^2.

LEDs were tested under constant current of 700 mA and the light efficiency is defined as the ratio of the output light energy to the input electrical energy. It can be seen that the light efficiency of both the blue and white LEDs increases with the PDD first and decreases after that. For the blue LEDs, a maximum light efficiency enhancement of ~10% was achieved at a wide range of PDD from 0.9 to 3.6 g/m^2. For the white LEDs, a maximum light efficiency enhancement of ~3.8% was achieved at PDD of ~0.9 g/m^2.

Fig. 7 illustrates the mechanism behind the light efficiency variation in LEDs with the PDD as shown in Fig. 6. For uncoated LEDs as shown in Fig. 7(a), most of the light is reflected at the flat silicone–air interface due to the refractive index difference of silicone (~1.53) and air, which induces severe light efficiency drop. When the nanoparticles deposit on and gradually cover the silicone film as shown in Fig. 7(b) and (c), the dome shape of the nanoparticles helps extract the light at the silicone–air interface, resulting in the increase in light efficiency. However, when the PDD further increases, the nanoparticles form layer-by-layer structure on most of the surface as shown in Fig. 7(d). The layer-by-layer structure reduces the light extraction efficiency due to the scattering and absorption of the nanoparticles. Furthermore, as shown in Fig. 7(b)–(d), part of the nanoparticles aggregate to form microscale structures. Each microscale structure contains thousands of nanoparticles with complicated layer-by-layer structure as shown in the SEM images of Fig. 7(d), which causes severe light scattering and absorption. The amount and size of the microscale structures increase with the PDD. As a result, the light efficiency decreases with the PDD after that.

The light efficiency of the blue LEDs mainly depends on the aggregate morphology of nanoparticles. For PDD < 0.9 g/m^2, the nanoparticles cover the silicone film gradually, which increases the light efficiency. When the PDD further increases, the nanoparticles aggregate and cover the silicone film simultaneously. The light efficiency enhancement of the nanoparticles makes up the light efficiency reduction caused by the nanoparticle aggregation. As a result, the light efficiency rarely changes with the PDD from 0.9 to 3.6 g/m^2. For PDD > 3.6 g/m^2, the particle aggregation becomes more serious. Therefore, the light efficiency decreases monotonously.

However, for the white LEDs with phosphor and QDs, the scattering and light absorption–conversion of the phosphor/QDs change the light propagation direction, which increases the light extraction efficiency [7]. As a result, the light efficiency enhancement by the nanoparticles is weakened. However, the light efficiency reduction by the aggregation of nanoparticles remains. Therefore, the light efficiency enhancement by the nanoparticles of the white LEDs is smaller than that of the blue LEDs. Besides, different from the blue LEDs, the light efficiency of the white LEDs increases when PDD < 0.9 g/m^2 and decreases after that.

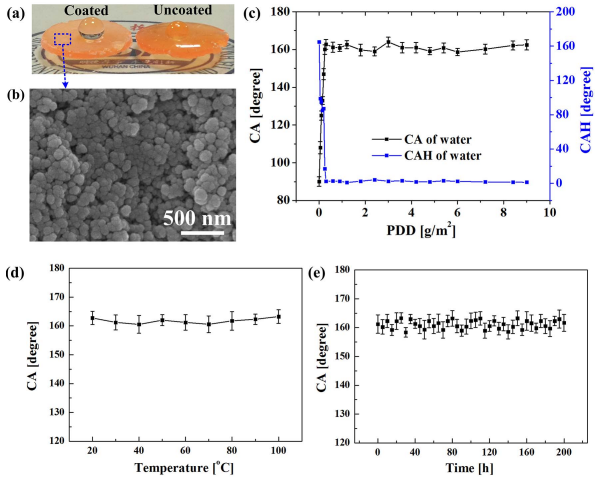

Fig. 8. Wettability characterization of the FOTS-NS-coated QDs/polymer films. (a) Wettability of the coated and uncoated films with the PDD of 0.9 g/m^2. (b) SEM image of the coated film. (c) CA and CAH of water droplets on the coated films with the PDD from 0 to 9 g/m^2. (d) Temperature dependence of CA of water droplets on the coated films with the PDD of 0.9 g/m^2 after heating for 100 h at fixed temperature. (e) Time evolution of CA of water droplets on the coated films with the PDD of 0.9 g/m^2 when immersing the films into 50 °C water pool.

The above results illustrate the effect of the FOTS-NS layer on the light efficiency of LEDs. To further investigate the effect of the FOTS-NS layer on the wettability and moisture stability of the QDs/polymer films, the FOTS-NS particles were coated on the QDs/polymer films with the PDD of 0–9 g/m^2. Fig. 8(a) shows the water droplets on the coated film with the PDD of 0.9 g/m^2 and uncoated film, and the diameter of the water droplet is ~2 mm. It can be seen that the coated film presents superhydrophobic property with water contact angle (CA) of ~160°, while the uncoated film shows hydrophilic property with water CA of ~85°. Fig. 8(c) shows the CA and CA hysteresis (CAH, difference between advancing CA and receding CA) of water droplets on the coated films with the PDD from 0 to 9 g/m^2. The CAs of the coated films are larger than 160° and the CAHs of the coated films are smaller than 2.5° when the PDD > 0.3 g/m^2, which indicates that the FOTS-NS layer can effectively prevent the water from penetrating the films with the PDD > 0.3 g/m^2. Moreover, the wettability and stability of the coated films with the PDD of 0.9 g/m^2 under heated and moisture conditions were characterized. For the heated condition test, the films were heated to a predefined temperature for 100 h before CA measurement, and the results are shown in Fig. 8(d). For the moisture condition test, the films were immersed into 50 °C water pool, and the CAs of the films over time are shown in Fig. 8(e). It can be seen that the CAs of the films almost keep constant under heated and moisture conditions, which prove the high wettability and stability of the films.

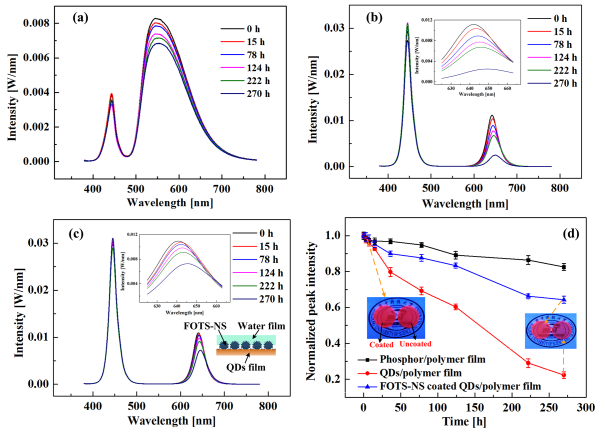

Fig. 9. Moisture stability characterization of the coated and uncoated films. (a) Spectra evolution of the phosphor/polymer films over aging time. (b) Spectra evolution of the QDs/polymer films over aging time. (c) Spectra evolution of the FOTS-NS-coated QDs/polymer films with the PDD of 0.9 g/m^2 over aging time. (d) Time evolution of the normalized peak intensity of films.

The moisture stability of the three types of samples shown in Fig. 3(b) was characterized with the experimental setup shown in Fig. 3(a). Based on the above results, the PDD of type 3 films was set as 0.9 g/m^2. Fig. 9(a)–(c) shows the spectra of the three types of samples over aging time. The intensity of the phosphor and QDs' emission spectra decrease as time goes by, which indicates the moisture induces irreversible fluorescence quenching of phosphor and QDs. Comparing Fig. 9(a) with (b), it can be seen that the QDs suffer more serious fluorescence quenching than the phosphor. Therefore, the moisture stability of the QDs will become the key parameter for deciding the reliability of the QDs-LEDs under moisture environment. Comparing Fig. 9(b) with (c), it can be seen that the spectra intensity degradation of the FOTS-NS-coated QDs/polymer film is much smaller than that of the uncoated QDs/polymer film, indicating that the moisture stability of the QDs is significantly enhanced with the FOTS-NS layer. To quantitatively characterize the moisture stability of phosphor and QDs, the normalized peak intensity of the phosphor and QDs' emission spectra was analyzed as shown in Fig. 9(c). It shows that the normalized peak intensity degradation of the phosphor/polymer films, QDs/polymer films, and FOTS-NS-coated QDs/polymer films after aging for 270 h is ∼17.43%, ∼77.66%, and ∼35.68%, respectively.

IV. Conclusion

In this article, we proposed a simple and feasible method to enhance the light efficiency and moisture stability of the QDs-LEDs. The superhydrophobic NS particles (FOTS-NS) were synthesized by modifying the pristine NS particles with 1H,1H,2H,2H-FOTS. The wettability of the FOTS-NS and the transparency of the FOTS-NS layer were characterized. The effect of the FOTS-NS layer on the light efficiency of the LEDs and the moisture stability of the QDs/polymer films was characterized. The results show that the FOTS-NS layers show high transparency and enhance the light efficiency of the LEDs by improving the light extraction efficiency at the silicone–air interface under low PDDs. Besides, the FOTS-NS particles form hierarchical structure to prevent the water from penetrating the QDs/polymer film, and thereby the FOTS-NS-coated films show higher moisture stability than the uncoated films.

References

[1] X. Luo, R. Hu, S. Liu, and K. Wang, "Heat and fluid flow in high-power LED packaging and applications," *Prog. Energy Combustion Sci.*, vol. 56, pp. 1–32, Sep. 2016.

[2] Y. C. Chi *et al.*, "Phosphorous diffuser diverged blue laser diode for indoor lighting and communication," *Sci. Rep.*, vol. 5, Nov. 2015, Art. no. 18690.

[3] Y.-F. Huang *et al.*, "LuAG: Ce/CASN: Eu phosphor enhanced high-CRI R/G/B LD lighting fidelity," *J. Mater. Chem. C*, vol. 7, no. 31, pp. 9556–9563, 2019.

[4] T. C. Wu *et al.*, "White-lighting communication with a $Lu_3Al_5O_{12}:Ce^{3+}$/$CaAlSiN_3:Eu^{2+}$ glass covered 450-nm InGaN laser diode," *J. Lightw. Technol.*, vol. 36, no. 9, pp. 1634–1643, May 1, 2018.

[5] X. Yu, W. Shu, R. Hu, B. Xie, Y. Ma, and X. Luo, "Dynamic phosphor sedimentation effect on the optical performance of white LEDs," *IEEE Photon. Technol. Lett.*, vol. 29, no. 14, pp. 1195–1198, Jul. 15, 2017.

[6] X. Yu, B. Xie, Q. Chen, Y. Ma, R. Wu, and X. Luo, "Thermal remote phosphor coating for phosphor-converted white-light-emitting diodes," *IEEE Trans. Compon., Packag., Manuf. Technol.*, vol. 5, no. 9, pp. 1253–1257, Sep. 2015.

[7] X. J. Yu, B. Xie, B. F. Shang, Q. Chen, and X. B. Luo, "A cylindrical tuber encapsulant geometry for enhancing optical performance of chip-on-board packaging light-emitting diodes," *IEEE Photon. J.*, vol. 8, no. 3, Jun. 2016, Art. no. 1600709.

[8] C.-C. Tsai, "Color rendering index thermal stability improvement of glass-based phosphor-converted white light-emitting diodes for solid-state lighting," *Int. J. Photoenergy*, vol. 2014, Jun. 2014, Art. no. 407239.

[9] C.-C. Tsai, W.-C. Cheng, G.-H. Chen, Y.-C. Lee, C. T. Kuo, and W.-H. Cheng, "High-color rendering indices performance of glass based phosphor-converted white light-emitting diodes for solid state lighting," *Proc. SPIE*, vol. 9003, Feb. 2014, Art. no. 90031K.

[10] B. Xie *et al.*, "Structural optimization for remote white light-emitting diodes with quantum dots and phosphor: Packaging sequence matters," *Opt. Express*, vol. 24, no. 26, pp. A1560–A1570, 2016.

[11] J. J. Zhang *et al.*, "Blue light hazard performance comparison of phosphor-converted LED sources with red quantum dots and red phosphor," *J. Appl. Phys.*, vol. 122, no. 4, 2017, Art. no. 043103.

[12] R. Wang, J. Zhang, X. Xu, Y. Wang, L. Zhou, and B. Li, "White LED with high color rendering index based on $Ca_8Mg(SiO_4)_4Cl_2:Eu^{2+}$ and ZnCdTe/CdSe quantum dot hybrid phosphor," *Mater. Lett.*, vol. 84, pp. 24–26, Oct. 2012.

[13] C. Y. Shen *et al.*, "High color rendering index white LED based on nano-YAG:Ce^{3+} phosphor hybrid with CdSe/CdS/ZnS core/shell/shell quantum dots," *J. Mod. Opt.*, vol. 59, no. 14, pp. 1199–1203, 2012.

[14] S. W. Buckner, R. L. Konold, and P. A. Jelliss, "Luminescence quenching in PbS nanoparticles," *Chem. Phys. Lett.*, vol. 394, nos. 4–6, pp. 400–404, 2004.

[15] M. Tata, S. Banerjee, V. T. John, Y. Waguespack, and G. L. McPherson, "Fluorescence quenching of CdS nanocrystallites in AOT water-in-oil microemulsions," *Colloids Surf. A, Physicochem. Eng. Aspects*, vol. 127, nos. 1–3, pp. 39–46, 1997.

[16] B. Xie *et al.*, "Targeting cooling for quantum dots in white QDs-LEDs by hexagonal boron nitride platelets with electrostatic bonding," *Adv. Funct. Mater.*, vol. 28, no. 30, 2018, Art. no. 1801407.

[17] M. J. Milla, J. M. Ulloa, and Á. Guzmán, "Strong influence of the humidity on the electrical properties of InGaAs surface quantum dots," *ACS Appl. Mater. Inter.*, vol. 6, no. 9, pp. 6191–6195, 2014.

[18] D. S. English, L. E. Pell, Z. Yu, P. F. Barbara, and B. A. Korgel, "Size tunable visible luminescence from individual organic monolayer stabilized silicon nanocrystal quantum dots," *Nano Lett.*, vol. 2, no. 7, pp. 681–685, 2002.

[19] B. Martín-garcía *et al.*, "Reduction of moisture sensitivity of PbS quantum dot solar cells by incorporation of reduced graphene oxide," *Solar Energy Mater. Solar Cells*, vol. 183, pp. 1–7, Aug. 2018.

[20] X. J. Zhang *et al.*, "Robust and stable narrow-band green emitter: An option for advanced wide-color-gamut backlight display," *Chem. Mater.*, vol. 28, no. 23, pp. 8493–8497, 2016.

[21] V. Malgras *et al.*, "Observation of quantum confinement in monodisperse methylammonium lead halide perovskite nanocrystals embedded in mesoporous silica," *J. Amer. Chem. Soc.*, vol. 138, no. 42, pp. 13874–13881, 2016.

[22] D. N. Dirin *et al.*, "Harnessing defect-tolerance at the nanoscale: Highly luminescent lead halide perovskite nanocrystals in mesoporous silica matrixes," *Nano Lett.*, vol. 16, no. 9, pp. 5866–5874, 2016.

[23] Y. Chen, M. Yu, S. Ye, J. Song, and J. Qu, "All-inorganic $CsPbBr_3$ perovskite quantum dots embedded in dual-mesoporous silica with moisture resistance for two-photon-pumped plasmonic nanoLasers," *Nanoscale*, vol. 10, no. 14, pp. 6704–6711, 2018.

[24] B. Xie *et al.*, "Realization of wide circadian variability by quantum dots-luminescent mesoporous silica-based white light-emitting diodes," *Nanotechnology*, vol. 28, no. 42, 2017, Art. no. 425204.

[25] Y.-T. Kwon *et al.*, "Synthesis of CdSe/ZnSe quantum dots passivated with a polymer for oxidation prevention," *Surf. Coat. Technol.*, vol. 259, pp. 83–86, Nov. 2014.

[26] H. Song and S. Lee, "Photoluminescent (CdSe) ZnS quantum dot–polymethylmethacrylate polymer composite thin films in the visible spectral range," *Nanotechnology*, vol. 18, no. 5, 2007, Art. no. 055402.

[27] J. Jang, S. Kim, and K. J. Lee, "Fabrication of CdS/PMMA core/shell nanoparticles by dispersion mediated interfacial polymerization," *Chem. Commun.*, vol. 26, pp. 2689–2691, 2007.

[28] H. Y. Kim *et al.*, "Quantum dot/siloxane composite film exceptionally stable against oxidation under heat and moisture," *J. Amer. Chem. Soc.*, vol. 138, no. 50, pp. 16478–16485, 2016.

[29] B. Xie *et al.*, "White light-emitting diodes with enhanced efficiency and thermal stability optimized by quantum dots-silica nanoparticles," *IEEE Trans. Electron Devices*, vol. 65, no. 2, pp. 605–609, Feb. 2018.

[30] B. Xie, R. Hu, X. Yu, B. Shang, Y. Ma, and X. Luo, "Effect of packaging method on performance of light-emitting diodes with quantum dot phosphor," *IEEE Photon. Technol. Lett.*, vol. 28, no. 10, pp. 1115–1118, May 15, 2016.

[31] B. Xie, R. Hu, and X. B. Luo, "Quantum dots-converted light-emitting diodes packaging for lighting and display: Status and perspectives," *J. Electron. Packag.*, vol. 138, Mar. 2016, Art. no. 020803.

[32] X. Luo, B. Wu, and S. Liu, "Effects of moist environments on LED module reliability," *IEEE Trans. Device Mater. Rel.*, vol. 10, no. 2, pp. 182–186, Jun. 2010.

[33] A. K. Kota, G. Kwon, and A. Tuteja, "The design and applications of superomniphobic surfaces," *NPG Asia Mater.*, vol. 6, no. 7, 2014, Art. no. e109.

[34] Y. Gao, Y. Huang, S. Feng, G. Gu, and F. L. Qing, "Novel superhydrophobic and highly oleophobic PFPE-modified silica nanocomposite," *J. Mater. Sci.*, vol. 45, no. 2, pp. 460–466, 2010.

[35] E. J. Park, D. H. Kim, J. H. Lee, S. Ha, C. Song, and Y. D. Kim, "Fabrication of a superhydrophobic and oleophobic PTFE membrane: An application to selective gas permeation," *Mater. Res. Bull.*, vol. 83, pp. 88–95, Nov. 2016.

[36] J.-J. Hao, J. Zhou, and C.-Y. Zhang, "A tri-n-octylphosphine-assisted successive ionic layer adsorption and reaction method to synthesize multilayered core–shell CdSe–ZnS quantum dots with extremely high quantum yield," *Chem. Commun.*, vol. 49, no. 57, pp. 6346–6348, 2013.

[37] X. Yu, B. Xie, B. Shang, W. Shu, and X. Luo, "A facile approach to fabricate patterned surfaces for enhancing light efficiency of COB-LEDs," *IEEE Trans. Electron Devices*, vol. 64, no. 10, pp. 4149–4155, Oct. 2017.

[38] X. Yu, R. Hu, R. Wu, B. Xie, X. Zhang, and X. Luo, "Cylindrical tuber encapsulant layer realization by patterned surface for chip-on-board light-emitting diodes packaging," *J. Electron. Packag.*, vol. 141, no. 3, 2019, Art. no. 031005.